

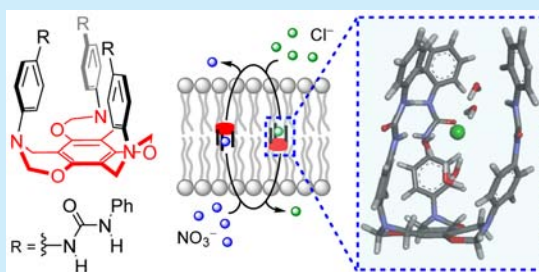
One-Pot Synthesis and Transmembrane Chloride Transport Properties of C<sub>3</sub>-Symmetric Benzoxazine Urea

Arundhati Roy, Debasis Saha, Arnab Mukherjee, and Pinaki Talukdar\*

Department of Chemistry, Indian Institute of Science Education and Research Pune, Dr. Homi Bhabha Road, Pashan, Pune, 411008 Maharashtra, India

## S Supporting Information

**ABSTRACT:** One-pot synthesis of a C<sub>3</sub>-symmetric benzoxazine-based tris-urea compound is discussed. <sup>1</sup>H NMR titrations indicate a stronger Cl<sup>−</sup> binding compared that of Br<sup>−</sup> and I<sup>−</sup> by the receptor. Effective Cl<sup>−</sup> transport across liposomal membranes via a Cl<sup>−</sup>/X<sup>−</sup> antiport mechanism is confirmed. Theoretical calculation suggests that a few water molecules with N–H, C=O, and the aromatic ring of the receptor create a H-bonded polar cavity where a Cl<sup>−</sup> is recognized by O–H⋯Cl<sup>−</sup> interactions from five bridged water molecules.



The transport of anions across the cell membrane plays a very crucial role in several biological processes such as signal transduction, control of intracellular pH, regulation of cell volume, stabilization of resting membrane potential, and fluid transport in epithelia.<sup>1</sup> Over the past decade, there has been an emerging interest in the design of small molecules that facilitate transmembrane anion transport, particularly chloride, bicarbonate, and sulfate.<sup>2</sup> This interest in synthetic chloride transporters has encouraged, mainly through the realization that misregulated chloride transport across cell membranes can lead to potential diseases (i.e., “channelopathies”), including cystic fibrosis, Dent’s disease, myotonia, epilepsy, etc.<sup>3</sup> Thus, it is very important to recognize the action of artificial transport systems to treat channelopathies, by overcoming the missing activities of natural transporters, and such a destined goal is still unfulfilled.<sup>4</sup> Therefore, designs of synthetic small molecules are progressively gaining pertinence, as these small molecules can mimic the activity and mechanism of transport of natural ionophores. Some of the synthetic anionophores are already recognized to have intriguing pharmacological activities as some of them have potential immunosuppressive, antimalarial, antineoplastic, and antimicrobial activities at concentrations below their cytotoxicity level to healthy cells.<sup>1b,5</sup>

Hydrogen-bond-forming ability of amide and urea is very important in supramolecular chemistry because these residues can be used in either self-assembly or ion recognition. Supramolecular assembly of these residues was applied to form ion channels where the cavity allowed either cation or water transport.<sup>6</sup> Adequate structural design based on amide and urea was useful in anion binding and transmembrane anion carrier formation.<sup>7</sup> Urea derivatives are superior in comparison to an amide as anion-recognizing residues due to more acidic N–H groups. Therefore, these groups were used further in the designs of dipodal and tripodal anion carriers to take the advantage of cooperative H-bonding interactions.<sup>7c,8</sup> However, the designs of

tripodal anion carriers with a high degree of preorganization are rare<sup>9</sup> and mostly constructed on a pre-existing rigid core moiety, such as cholic acid.<sup>8c,d</sup> We, on the other hand, aimed to design new tripodal anion transporters by the facile construction of the rigid core. This strategy was envisaged to allow efficient synthesis and manipulation of transport activity based on the selection of recognizing arms. Herein, we report the design, synthesis, and ion transport behavior of new tripodal receptors **1** and **2** based on the C<sub>3</sub>-symmetric benzoxazine core and anion-recognizing arms composed of either amide or urea moieties (Figure 1A). As stated

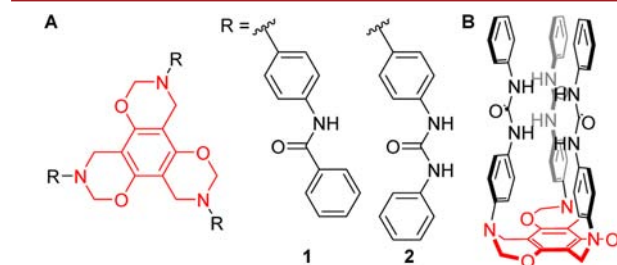


**Figure 1.** Structures of C<sub>3</sub>-symmetric tripodal receptors **1** and **2** (A). Representation of the anion binding cavity of **2** (B).

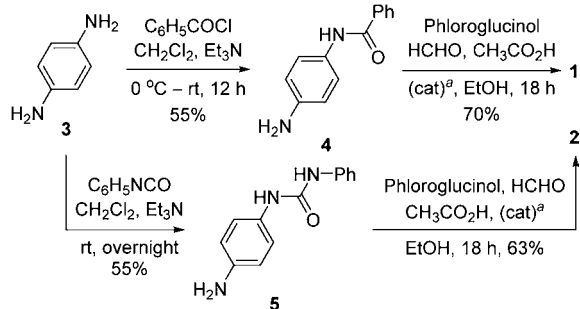
above, the tris-urea-based receptor **2** was predicted to be a better anion receptor compared to the tris-amide-based receptor **1** because it has more acidic N–H groups (Figure 1B).

Syntheses of molecules **1** and **2** were initiated from *p*-phenylenediamine **3** (Scheme 1). Compound **3** was converted to amide **4** in 55% yield upon reaction with benzoyl chloride.<sup>10</sup> Amide **4** was then reacted with phloroglucinol in the presence of formaldehyde and a catalytic amount of acetic acid in EtOH following the protocol reported by Singh et al.<sup>11</sup> to obtain

Received: September 29, 2016

Published: October 28, 2016

## Scheme 1. Synthesis of Tripodal Receptors 1 and 2

<sup>a</sup>Catalytic amount.

receptor 1 in 70% yield. In this step, each arm was linked to the core through the Mannich aminomethylation and a sequential ring closure condensation. Synthesis of the urea arm 5 was done in 55% yield by treating 3 with phenylisocyanate in  $\text{CH}_2\text{Cl}_2$ .<sup>12</sup> Reaction of 5, phloroglucinol, formaldehyde, and a catalytic amount of acetic acid in EtOH provided tripodal urea 2 in 63% yield.

The  $\text{Cl}^-$  binding with receptors 1 and 2 was evaluated by  $^1\text{H}$  NMR spectroscopy in  $\text{DMSO}-d_6$ .<sup>13</sup> Upon addition of tetrabutylammonium chloride (TBACl), a significant downfield shift ( $\Delta\delta \sim 0.8$  ppm) of N–H signals was observed for urea receptor 2 (Figures 2 and S4) while a corresponding change for

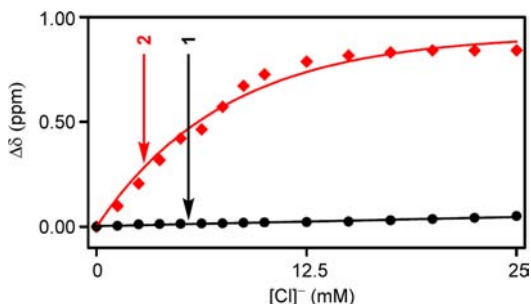


**Figure 2.** Shift of the N–H protons of receptors 1 and 2 upon addition of TBACl in  $\text{DMSO}-d_6$ .

amide receptor 1 was negligible (Figure S1). Job plot analysis<sup>14</sup> for 2 provided 1:1 (host/guest) stoichiometry (Figure S8), and subsequently, the stability constant<sup>15</sup> =  $335 \text{ M}^{-1}$  was determined (Figure S4) by fitting in the 1:1 model of the WineQNMR program (Figure S9). However, very weak and negligible binding was observed for 2 with TBABr (Figure S5) and TBAI (Figure S6), respectively. For receptor 1, the binding constants with  $\text{Cl}^-$ ,  $\text{Br}^-$ , and  $\text{I}^-$  could not be determined because of insignificant changes observed for the N–H protons (Figures S1–S3). These results indicate much stronger bonding of 2 compared to 1 with  $\text{Cl}^-$  due to the presence of the higher number of hydrogen-bond donor groups in this system.

Ion transport properties of compounds 1 and 2 across large unilamellar vesicles (LUVs), prepared from egg yolk phosphatidylcholine (EYPC) lipid encapsulated with pH-sensitive fluorescent dye 8-hydroxypyrene-1,3,6-trisulfonate (HPTS),<sup>5a,16</sup> were determined by applying a pH gradient,  $\Delta\text{pH} = 0.8$  ( $\text{pH}_{\text{in}} = 7.0$  and  $\text{pH}_{\text{out}} = 7.8$ ). Upon addition of each compound, the transport activity was measured through the collapse of the applied pH gradient, that is, via either  $\text{H}^+$  efflux or  $\text{OH}^-$  influx (Figure S10). Ion transport activity of receptor 2 was

found to be superior to that of receptor 1 (Figure 3A). The concentration-dependent ion transport ability of 2 (Figure 3B)

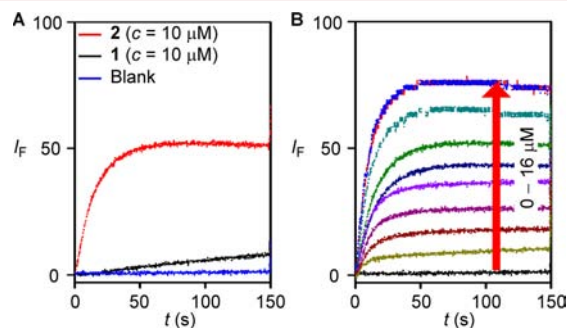


**Figure 3.** Comparison of ion transport activity for receptors 1 and 2 (A), concentration profile of receptor 2, presented as a function of time with their normalized emission intensity,  $I_F$  (B). Color codes: black,  $0 \mu\text{M}$ ; olive green,  $2 \mu\text{M}$ ; burgundy,  $4 \mu\text{M}$ ; magenta,  $6 \mu\text{M}$ ; purple,  $8 \mu\text{M}$ ; dark blue,  $10 \mu\text{M}$ ; green,  $12 \mu\text{M}$ ; blue/green,  $14 \mu\text{M}$ ; red,  $15 \mu\text{M}$ ; blue,  $16 \mu\text{M}$ .

provided  $\text{EC}_{50} = 8.2 \mu\text{M}$  and Hill coefficient  $n = 1.4$  (Figure S11) when dose–response analysis was carried out with a concentration-dependent assay using normalized values at  $t = 10$  s. These data indicated that one molecule of 2 is involved in the active structure formation. For 1, the Hill coefficient could not be obtained due to its low activity.

Based on the aforementioned ion transport activity of receptor 2, its ability to discriminate among different ions was evaluated across EYPC LUVs with entrapped HPTS.<sup>17</sup> Replacement of the extravesicular  $\text{NaCl}$  with iso-osmolar  $\text{MCl}$  ( $\text{M}^+ = \text{Li}^+$ ,  $\text{K}^+$ ,  $\text{Rb}^+$ , and  $\text{Cs}^+$ ) did not cause any significant change in the transport activity of 2 (Figure 4A). However, the changes provoked by

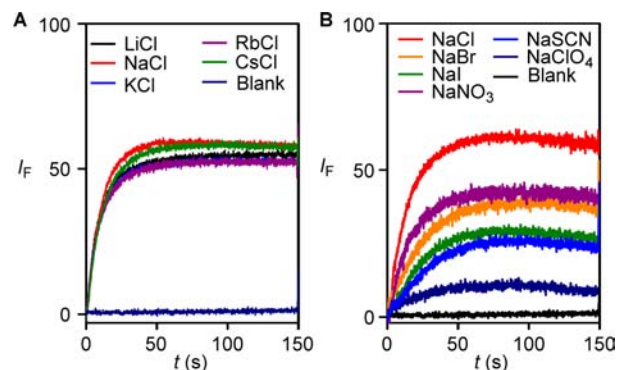


**Figure 4.** Effect of extravesicular cations (A) and anions (B) on ion transport by 2 across EYPC LUVs with entrapped HPTS.

different iso-osmolar extravesicular anions  $\text{NaX}$  ( $\text{X}^- = \text{Cl}^-$ ,  $\text{Br}^-$ ,  $\text{I}^-$ ,  $\text{NO}_3^-$ ,  $\text{SCN}^-$ ,  $\text{ClO}_4^-$ ) exchange were clearly stronger (Figure 4B) with the selectivity sequence  $\text{Cl}^- > \text{NO}_3^- > \text{Br}^- > \text{I}^- > \text{SCN}^- > \text{ClO}_4^-$ . The observed selectivity sequence for an anion could be the outcome of several processes such as (1)  $\text{OH}^-/\text{Cl}^-$  exchange or  $\text{H}^+/\text{Cl}^-$  co-transport due to pH gradient; (2)  $\text{Cl}^-/\text{X}^-$  exchange induced by anion gradient, followed by  $\text{OH}^-/\text{X}^-$  exchange or  $\text{H}^+/\text{X}^-$  co-transport encouraged by pH gradient, and (3)  $\text{OH}^-/\text{X}^-$  exchange or  $\text{H}^+/\text{X}^-$  co-transport against the pH gradient. To determine the correct mechanism, ion transport studies were done with identical intravesicular and extravesicular buffer solution by varying only the anions (Figure S12B). The observed data suggest the same selectivity sequence ( $\text{Cl}^- > \text{NO}_3^-$

$> \text{Br}^- > \text{I}^- > \text{SCN}^- > \text{ClO}_4^-$ ), ruling out all other possibilities and establishing  $\text{OH}^-/\text{X}^-$  exchange as the primary transport mechanism.

To gain additional evidence of  $\text{Cl}^-$  selectivity of **2**,  $\text{Cl}^-$  leakage studies were performed across EYPC LUVs with entrapped lucigenin dye.<sup>7c,18</sup> With iso-osmolar intra- and extravesicular  $\text{NaNO}_3$  (200 mM), an external pulse of  $\text{NaCl}$  (25 mM) was applied. The influx of  $\text{Cl}^-$  upon addition of **2** was monitored through the decay in lucigenin fluorescence. Compound **2** showed a concentration-dependent enhancement of  $\text{Cl}^-$  influx **2** (Figure 5A), and the initial rate  $I_R = 0.026 \text{ s}^{-1}$  and half-life  $t_{1/2} =$

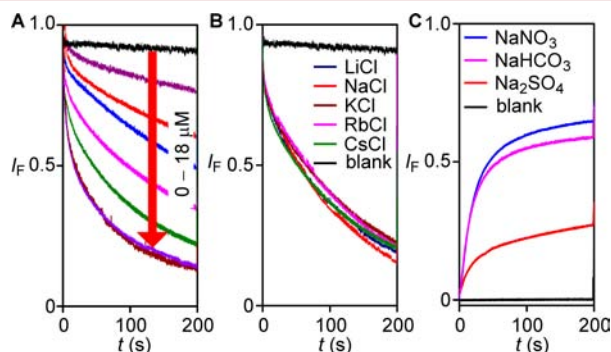


**Figure 5.**  $\text{Cl}^-$  influx by **2** across EYPC LUVs with entrapped lucigenin (A). Color codes: black, 0  $\mu\text{M}$ ; dark purple, 5  $\mu\text{M}$ ; red, 8  $\mu\text{M}$ ; blue, 10  $\mu\text{M}$ ; bright pink, 12  $\mu\text{M}$ ; green, 14  $\mu\text{M}$ ; purple, 16  $\mu\text{M}$ ; burgundy, 18  $\mu\text{M}$ . Effect of extravesicular cations on  $\text{Cl}^-$  influx by **2** (B). Effect of extravesicular anions on  $\text{Cl}^-$  efflux by **2** (C).

57 s calculated at 14  $\mu\text{M}$  concentration indicated fast  $\text{Cl}^-$  transport by **2**. Initial rates at other concentrations are provided in the Supporting Information. Replacement of extravesicular  $\text{Na}^+$  with  $\text{M}^+ = \text{Li}^+, \text{Na}^+, \text{K}^+, \text{Rb}^+, \text{and } \text{Cs}^+$  provided no significant change in  $\text{Cl}^-$  influx rate (Figure 5B), suggesting that the  $\text{M}^+/\text{Cl}^-$  symport mechanism is not operative during the ion transport by **2**. To understand the effect of anions, LUVs prepared with  $\text{NaCl}$  (200 mM) were dispersed in  $\text{NaX}$  (200 mM,  $\text{X}^- = \text{NO}_3^-, \text{HCO}_3^-, \text{and } \text{SO}_4^{2-}$ ) and **2** was added. In this study, clear changes in the  $\text{Cl}^-$  efflux rates were observed (Figure 5C). The resulting trend correlates to the  $\text{Cl}^-/\text{X}^-$  antiport as the main transport mechanism for the transport activity of **2**. The  $\text{Cl}^-$  transport by **2** was further studied in the presence of valinomycin, an efficient  $\text{K}^+$  carrier.<sup>19</sup> LUVs were prepared from EYPC with entrapped lucigenin (1 mM) and iso-osmolar intra- and extravesicular  $\text{NaNO}_3$  (200 mM). Subsequently, an extravesicular  $\text{KCl}$  (25 mM) pulse was applied prior to each experiment. Addition of valinomycin (100 nM) did not show any quenching of lucigenin fluorescence. However, **2** (10  $\mu\text{M}$ ), in the presence of valinomycin (100 nM), exhibited significant quenching of lucigenin fluorescence as compared to quenching caused by **2** (10  $\mu\text{M}$ ) alone (Figure S14). These results further support that **2** is an effective anion antiporter.

The direct experimental evidence of  $\text{Cl}^-$  binding by **2** was obtained by electrospray ionization mass spectrometric (ESI-MS) studies in the negative mode. In this experiment, solutions of compound **2** (10  $\mu\text{M}$ ) in  $\text{CH}_3\text{CN}$  were mixed (in 1:3, 1:2, 1:1, 2:1, 3:1 molar ratios) and ESI-MS was recorded. Each set showed  $m/z = 914.3359$ , which corresponds to the adduct **2** +  $\text{Cl}^-$ , confirming 1:1  $\text{Cl}^-$  binding (Figure S16). Evidence of the mobile carrier mechanism was derived from the U-tube experiment using chloroform as an organic phase separating two aqueous phases, one containing  $\text{Cl}^-$  (in the source arm) and the other

with  $\text{NO}_3^-$  salt (in the receiving arm). Significant  $\text{Cl}^-$  transport to the receiving arm, observed by monitoring the ion concentration with a chloride-selective electrode for 6 days, indicated that **2** can operate via a mobile carrier mechanism (Figure S15).

To determine the  $\text{Cl}^-$ -bound structure of the molecule, the molecule was initially optimized along with a  $\text{Cl}^-$  ion using the semiempirical PM6 method<sup>20</sup> in the Gaussian 09 program package.<sup>21</sup> The optimized structure was then inserted inside a pre-equilibrated 1,2-dipalmitoyl-*sn*-phosphocholine (DPPC)/water lipid bilayer system. Initially, position restraint was applied to **2** and the  $\text{Cl}^-$  ion, and the system was equilibrated for 1 ns at constant temperature and pressure. Then the restraint was removed, and a 5 ns long simulation was carried out at same conditions. The other simulation details are given in the Supporting Information. From analyzing the last 1 ns of the 5 ns trajectory, we found that the  $\text{Cl}^-$  remained bound to the molecule with an average of five water molecules within 4 Å of the ion. The overall structure of the simulation box is shown in Figure 6A. From cluster analysis of the 1 ns trajectory, the  $\text{Cl}^-$ -

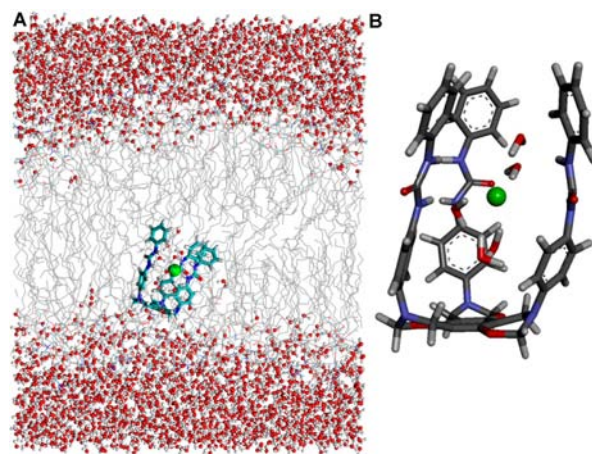


**Figure 6.** Equilibrated system with compound **2** inserted in the DPPC lipid layer along with the bound  $\text{Cl}^-$  ion (A). The  $\text{Cl}^-$ -bound structure of **2** along with the H-bonded water molecules with side view obtained from MD simulation (B).

bound structure is obtained where five water molecules were found to form H-bonds with the  $\text{Cl}^-$  ion. The water molecules also form a H-bonded network, supported by the H-bonding with N–H, C=O, and aromatic ring of the molecule (Figures 6B and S17C).

In conclusion, we have developed new class of tripodal tris-amide- and tris-urea-based receptors which can mediate  $\text{Cl}^-$  transport across large unilamellar vesicles. These receptors were designed on a benzoxazine core and synthesized in one pot with Mannich aminomethylation and a sequential ring closure condensation to connect each arm.  $^1\text{H}$  NMR titrations in  $\text{DMSO}-d_6$  revealed that the tris-urea is better as a  $\text{Cl}^-$  ion binding receptor in comparison to the tris-amide derivative, and it also forms a 1:1 complex with the ion. Importantly, it was found that the tris-urea compound is also a more effective anion carrier with a selectivity sequence of  $\text{Cl}^- > \text{NO}_3^- > \text{Br}^- > \text{I}^- > \text{SCN}^- > \text{ClO}_4^-$ , and the antiport mechanism during anion transport was also established. Molecular dynamics simulation suggests that the  $\text{Cl}^-$  ion binds to the polar cavity of the receptor assisted by hydrogen bonding from a few water molecules, which in turn forms

hydrogen bonds to the polar groups of the receptor and among themselves.

## ■ ASSOCIATED CONTENT

### Supporting Information

The Supporting Information is available free of charge on the ACS Publications website at DOI: 10.1021/acs.orglett.6b02940.

General methods and measurements (PDF)

## ■ AUTHOR INFORMATION

### Corresponding Author

\*E-mail: ptalukdar@iiserpune.ac.in.

### Notes

The authors declare no competing financial interest.

## ■ ACKNOWLEDGMENTS

We acknowledge the Director, IISER Pune, and SERB, Govt. of India (Grant Nos. EMR/2014/000873B and EMR/2016/001069) for research funding. A.R. thanks the University Grant Commission for research fellowship.

## ■ REFERENCES

- (1) (a) Jentsch, T. J.; Stein, V.; Weinreich, F.; Zdebik, A. A. *Physiol. Rev.* **2002**, *82*, 503–568. (b) Ko, S.-K.; Kim, S. K.; Share, A.; Lynch, V. M.; Park, J.; Namkung, W.; Van Rossom, W.; Busschaert, N.; Gale, P. A.; Sessler, J. L.; Shin, I. *Nat. Chem.* **2014**, *6*, 885–892. (c) DeCoursey, T. E.; Chandy, K. G.; Gupta, S.; Cahalan, M. D. *Nature* **1984**, *307*, 465–468.
- (2) (a) Matile, S.; Vargas Jentzsch, A.; Montenegro, J.; Fin, A. *Chem. Soc. Rev.* **2011**, *40*, 2453–2474. (b) Davis, J. T.; Okunola, O.; Quesada, R. *Chem. Soc. Rev.* **2010**, *39*, 3843–3862. (c) Gale, P. A. *Acc. Chem. Res.* **2011**, *44*, 216–226. (d) Elie, C.-R.; Noujeim, N.; Pardin, C.; Schmitzer, A. R. *Chem. Commun.* **2011**, *47*, 1788–1790.
- (3) Ohkuma, S.; Sato, T.; Okamoto, M.; Matsuya, H.; Arai, K.; Kataoka, T.; Nagai, K.; Wasserman, H. H. *Biochem. J.* **1998**, *334*, 731–741.
- (4) Jentsch, T. J.; Hubner, C. A.; Fuhrmann, J. C. *Nat. Cell Biol.* **2004**, *6*, 1039–1047.
- (5) (a) Saha, T.; Hossain, M. S.; Saha, D.; Lahiri, M.; Talukdar, P. J. *Am. Chem. Soc.* **2016**, *138*, 7558–7567. (b) Soto-Cerrato, V.; Manuel-Manresa, P.; Hernando, E.; Calabuig-Fariñas, S.; Martínez-Romero, A.; Fernández-Dueñas, V.; Sahlholm, K.; Knöpfel, T.; García-Valverde, M.; Rodilla, A. M.; Jantus-Lewintre, E.; Farràs, R.; Ciruela, F.; Pérez-Tomás, R.; Quesada, R. *J. Am. Chem. Soc.* **2015**, *137*, 15892–15898.
- (6) (a) Gilles, A.; Barboiu, M. *J. Am. Chem. Soc.* **2016**, *138*, 426–432. (b) Licsandru, E.; Kocsis, I.; Shen, Y.-x.; Murail, S.; Legrand, Y.-M.; van der Lee, A.; Tsai, D.; Baaden, M.; Kumar, M.; Barboiu, M. *J. Am. Chem. Soc.* **2016**, *138*, 5403–5409. (c) Le Duc, Y.; Michau, M.; Gilles, A.; Gence, V.; Legrand, Y.-M.; van der Lee, A.; Tingry, S.; Barboiu, M. *Angew. Chem., Int. Ed.* **2011**, *50*, 11366–11372.
- (7) (a) Davis, J. T.; Gale, P. A.; Okunola, O. A.; Prados, P.; Iglesias-Sánchez, J. C.; Torroba, T.; Quesada, R. *Nat. Chem.* **2009**, *1*, 138–144. (b) Wenzel, M.; Light, M. E.; Davis, A. P.; Gale, P. A. *Chem. Commun.* **2011**, *47*, 7641–7643. (c) Busschaert, N.; Wenzel, M.; Light, M. E.; Iglesias-Hernández, P.; Pérez-Tomás, R.; Gale, P. A. *J. Am. Chem. Soc.* **2011**, *133*, 14136–14148. (d) Hussain, S.; Brotherhood, P. R.; Judd, L. W.; Davis, A. P. *J. Am. Chem. Soc.* **2011**, *133*, 1614–1617.
- (8) (a) Busschaert, N.; Gale, P. A.; Haynes, C. J. E.; Light, M. E.; Moore, S. J.; Tong, C. C.; Davis, J. T.; Harrell, W. A. *Chem. Commun.* **2010**, *46*, 6252–6254. (b) Cooper, J. A.; Street, S. T. G.; Davis, A. P. *Angew. Chem., Int. Ed.* **2014**, *53*, 5609–5613. (c) Edwards, S. J.; Valkenier, H.; Busschaert, N.; Gale, P. A.; Davis, A. P. *Angew. Chem., Int. Ed.* **2015**, *54*, 4592–4596. (d) Clare, J. P.; Ayling, A. J.; Joos, J.-B.; Sisson, A. L.; Magro, G.; Pérez-Payán, M. N.; Lambert, T. N.; Shukla, R.; Smith, B. D.; Davis, A. P. *J. Am. Chem. Soc.* **2005**, *127*, 10739–10746.
- (9) Busschaert, N.; Karagiannidis, L. E.; Wenzel, M.; Haynes, C. J. E.; Wells, N. J.; Young, P. G.; Makuc, D.; Plavec, J.; Jolliffe, K. A.; Gale, P. A. *Chem. Sci.* **2014**, *5*, 1118–1127.
- (10) Hie, L.; Fine Nathel, N. F.; Shah, T. K.; Baker, E. L.; Hong, X.; Yang, Y.-F.; Liu, P.; Houk, K. N.; Garg, N. K. *Nature* **2015**, *524*, 79–83.
- (11) Singh, R.; Schober, M.; Hou, X.; Seay, A.; Chu, Q. *Tetrahedron Lett.* **2012**, *53*, 173–175.
- (12) Rodríguez, F.; Rozas, I.; Kaiser, M.; Brun, R.; Nguyen, B.; Wilson, W. D.; García, R. N.; Dardonville, C. *J. Med. Chem.* **2008**, *51*, 909–923.
- (13) (a) Cranwell, P. B.; Hiscock, J. R.; Haynes, C. J. E.; Light, M. E.; Wells, N. J.; Gale, P. A. *Chem. Commun.* **2013**, *49*, 874–876. (b) Haynes, C. J. E.; Berry, S. N.; Garric, J.; Herniman, J.; Hiscock, J. R.; Kirby, I. L.; Light, M. E.; Perkes, G.; Gale, P. A. *Chem. Commun.* **2013**, *49*, 246–248. (c) Busschaert, N.; Elmes, R. B. P.; Czech, D. D.; Wu, X.; Kirby, I. L.; Peck, E. M.; Hendzel, K. D.; Shaw, S. K.; Chan, B.; Smith, B. D.; Jolliffe, K. A.; Gale, P. A. *Chem. Sci.* **2014**, *5*, 3617–3626.
- (14) Saeed, M. A.; Fronczek, F. R.; Hossain, M. A. *Chem. Commun.* **2009**, 6409–6411.
- (15) Hynes, M. J. *J. Chem. Soc., Dalton Trans.* **1993**, 311–312.
- (16) (a) Vargas Jentzsch, A.; Emery, D.; Mareda, J.; Metrangola, P.; Resnati, G.; Matile, S. *Angew. Chem., Int. Ed.* **2011**, *50*, 11675–11678. (b) Sakai, N.; Matile, S. *J. Am. Chem. Soc.* **2003**, *125*, 14348–14356.
- (17) (a) Gorteau, V.; Bollot, G.; Mareda, J.; Perez-Velasco, A.; Matile, S. *J. Am. Chem. Soc.* **2006**, *128*, 14788–14789. (b) Talukdar, P.; Bollot, G.; Mareda, J.; Sakai, N.; Matile, S. *J. Am. Chem. Soc.* **2005**, *127*, 6528–6529.
- (18) (a) Choi, Y. R.; Chae, M. K.; Kim, D.; Lah, M. S.; Jeong, K.-S. *Chem. Commun.* **2012**, *48*, 10346–10348. (b) Lisbjerg, M.; Valkenier, H.; Jessen, B. M.; Al-Kerdi, H.; Davis, A. P.; Pittelkow, M. *J. Am. Chem. Soc.* **2015**, *137*, 4948–4951.
- (19) Shang, J.; Si, W.; Zhao, W.; Che, Y.; Hou, J.-L.; Jiang, H. *Org. Lett.* **2014**, *16*, 4008–4011.
- (20) Stewart, J. J. P. *J. Mol. Model.* **2007**, *13*, 1173–1213.
- (21) Frisch, M. J.; et al. *Gaussian 09*, revision C01, Gaussian, Inc.: Wallingford, CT, 2009.